NEOPLASIA
www.neoplasia.com

Volume 19 Number 4 April 2017 pp. 354–363 354

ABT-737 Synergizes with Cisplatin Bypassing Aberration of Apoptotic Pathway in Non-small Cell Lung Cancer

Eun Young Kim*, Ji Ye Jung*, Arum Kim†, Yoon Soo Chang† and Se Kyu Kim*

*Department of Internal Medicine, 3rd Floor, Yonsei University College of Medicine, 50-1 Yonsei-ro, Seodaemun-gu, 03722, Seoul, Rep of Korea; †Department of Internal Medicine, 8th Floor Annex Bldg, Gangnam Severance Hospital, Yonsei University College of Medicine, 211-Eonju-ro, Gangnam-gu, 06273, Seoul, Rep of Korea

Abstract

A subset of non-small cell lung cancer (NSCLC), which does not have a druggable driver mutation, is treated with platinum-based cytotoxic chemotherapy, but it develops resistance triggered by DNA damage responses. Here, we investigated the effect of activation of STAT3 by cisplatin on anti-apoptotic proteins and the effectiveness of a co-treatment with cisplatin and a BH3 mimetic, ABT-737. We analyzed the relationship between cisplatin and STAT3 pathway and effect of ABT-737, when combined with cisplatin in NSCLC cells and K-ras mutant mouse models. The synergism of this combination was evaluated by the Chou-Talalay Combination Index method. In *vivo* activity was evaluated by micro-CT. In NSCLC cells, there was a time and dose-dependent phosphorylation of SRC-JAK2-STAT3 by cisplatin, followed by increased expression of anti-apoptotic molecules. When the expression of the BCL-2 protein family members was evaluated in clinical samples, BCL-xL was most frequently overexpressed. Dominant negative STAT3 suppressed their expression, suggesting that STAT3 mediates cisplatin mediated overexpression of the anti-apoptotic molecules. ABT-737 displaced BCL-xL from mitochondria and induced oligomerization of BAK. ABT-737 itself showed cytotoxic effects and a combination of ABT-737 with cisplatin showed strong synergistic cytotoxicity. In a murine lung cancer model, co-treatment with ABT-737 and cisplatin induced significant tumor regression. These findings reveal a synergistic cytotoxic and anti-tumor activity of ABT-737 and cisplatin co-treatment in preclinical models, and suggest that clinical trials using this strategy may be beneficial in advanced NSCLC.

Neoplasia (2017) 19, 354–363

Introduction

Lung cancer is a common and leading cause of cancer death worldwide. In the year 2012, 1,824,701 new lung cancer were diagnosed, and 1,590,000 patients died of this devastating disease worldwide [1]. Advanced stage of lung cancer, which does not have a druggable driver mutation, is treated with platinum based-cytotoxic chemotherapy, but clinical outcome is suboptimal.

Cisplatin is a prototypic platinum chemotherapeutic agent and one of the most commonly prescribed drugs for the treatment of solid malignancies; however, its therapeutic benefits are often limited because of multiple resistance mechanisms. These resistance mechanisms can be classified by the alterations of steps (1) delivering cisplatin to DNA (pre-target resistance), (2) forming DNA-cisplatin adducts (on-target resistance) (3) related to cell death pathways elicited by DNA damage responses (post-target resistance) and (4) affecting signaling pathways that do not have obvious links with cisplatin treatment (off-target resistance) [2].

Overexpression of antiapoptotic members of the BCL-2 protein family is a cause for poor responses to chemotherapeutic agents and is

Abbreviations: CI, combination index; DFS, disease-free survival; FFPE, formalin-fixed paraffin embedded; IHC, immunohistochemistry; MTT, 3-(4,5-dimethylthiazol-2-yl)-2,5-diphenyltetrazolium bromide; NSCLC, non-small cell lung cancer; OS, overall survival; RT-PCR, real-time PCR.

Address all correspondence to: YS Chang.
E-mail: yschang@yuhs.ac

Received 8 December 2016; Revised 10 February 2017; Accepted 15 February 2017

1476-5586
http://dx.doi.org/10.1016/j.neo.2017.02.008

related to cisplatin resistance and diseases recurrence in cancer [3,4]. Alterations in cell death pathway induced by DNA damage responses is one of the critical mechanisms related to chemoresistance, and therefore, modulation or bypass of these responses might be an effective way in improving treatment outcomes [5,6]. Influence of MAPK pathway activation on cisplatin mediated apoptotic pathway is well established, but the relationship between JAK2-STAT3 pathway and response to cisplatin mediated cytotoxicity is limited (7). Considering the role of STAT3 as an oncogene and that activation of its signaling confers resistance to apoptosis, it is important to identify the relationship and to develop effective control modality.

Inactivation of BCL-2 family proteins might overcome the resistance against cisplatin-mediated apoptosis and may improve clinical outcomes. BH3-only proteins of BCL-2 family can directly or indirectly activate the effector protein of the mitochondrial membrane permeabilization. In the indirect (displacement) model, the BH3-only proteins (NOXA, BAD and BIM) insert their a-helical BH3 domain into the hydrophobic groove of prosurvival proteins. In the direct activation model, BH3-only proteins are classified into "sensitizer" and "activator". In this model, the activator BH3-only proteins (BIM, tBID) are sequestered by prosurvival proteins. The subsequent interaction between the prosurvival proteins and "sensitizer" BH3-only proteins (BAD, NOXA) releases the "activator" proteins [7]. In both model, the binding of BH3-only proteins to prosurvival molecules results in BAX/BAK conformation change, oligomerization and mitochondrial membrane permeabilization [8,9]. BH3 mimetics show a biochemical affinity for specific anti-apoptotic BCL-2 proteins and this is linked to their ability to kill specific cells. Several clinical trials have been performed using BH3 mimetics, such as ABT-737, ABT-263, AT-101, GX15-070, and TW-37, with limited success [10]. We hypothesize that a combination of cisplatin with prototypic BH3 mimetics, ABT-737, would overcome the cisplatin resistance caused by STAT3 activation.

In this study, we investigated the relationship between cisplatin and STAT3 pathway and effect of ABT-737, prototype of BH3 mimetics, when combined with cisplatin in non-small cell lung cancer (NSCLC) cells and a *K-ras* mutant mouse models. The synergism of this combination was evaluated by the Chou-Talalay Combination Index (CI) method. *In vivo* activity was evaluated by microCT and showed that this combination can be effectively applied for the treatment of lung cancer.

Materials and Methods

Cell Lines, Plasmids, Clinical Specimens, Chemicals, and Antibodies

A549 and H1703 cells were purchased from ATCC (Manassas, VA, USA) in 2012. H460, H1299, H358, H2009, and H596 cells were obtained from the Korean Cell Line Bank in 2012 (https://cellbank.snu.ac.kr/main/, Seoul, Korea), which provides cell test and authentication by DNA fingerprinting analysis by short tandem repeat markers and mycoplasma contamination test. Except for the experiment for revision, cells were used within six months after purchase. EF.GFP (#17616), EF.STAT3DN.Ubc.GFP (#24984), pCDNA3 Flag MKK7B2Jnk1a1 (#19726), and, pCDNA3 Flag MKK7B2Jnk1a1(APF) (#19730), were obtained from Addgene (Cambridge, MA, USA) and pcDNA3 were obtained from Invitrogen (Carlsbad, CA, USA). Anisomycin (ab120495) was purchased from Abcam (Cambridge, UK) and dasatinib (# S1021) was purchased from Selleckchem (Houston, TX, USA). To evaluate expression of anti-apoptotic proteins in human NSCLC, 12-paired lysates from adjacent normal appearing lung tissue and cancer-enriched tissue were analyzed by immunoblotting. Another set of 117 formalin-fixed paraffin embedded (FFPE) NSCLC tissue were used for immunohistochemistry (IHC). This study was approved by the IRB of Gangnam Severance Hospital (IRB #3–2014-0299) and was carried out in accordance with the Declaration of Helsinki and Korean GCP guidelines. ABT-737 was purchased from the AdooQ™ Bioscience (Irvine, CA, USA) and its chemical and crystal structure was described in elsewhere [11,12]. Antibodies, unless otherwise stated, were obtained from Cell Signaling Technology (Danvers, MA, USA).

Immunoblotting

Cells were harvested on ice using 2×Laemmli sample buffer containing protease and phosphatase inhibitors (Sigma-Aldrich). After sonication, 30–50 mg of lysate was separated by gel electrophoresis on 7.5 to 12% polyacrylamide gels and transferred onto nitrocellulose membranes (Bio-Rad Laboratories, Inc., Richmond, CA, USA). The expression level of each protein was measured using ImageJ (http://rsbweb.nih.gov/ij/) and quantified relative to that of β-actin [5].

RT-PCR

The RT-PCR was performed as described elsewhere [13]. Total RNA was extracted using TRI reagent (Ambion, Austin, TX, USA). Quantitative RT-PCR analysis was performed using TaqMan Gene Expression assay reagents and the StepOnePlus Real-Time PCR system (Applied Biosystems, Carlsbad, CA, USA) using an inventoried primer-probe set (http://bioinfo.appliedbiosystems.com/genome-database/gene-expression.html).

Mitochondrial Cytochrome c Release Assay

Cells were harvested and suspended in cell permeability buffer and incubated on ice for 10 minutes [14]. Cell disruption was performed by pipetting and vortexing. The homogenates were spun at 700×*g* for 10 min at 4°C. The supernatants were transferred to a fresh tube and spun at 13,000×*g* for 10 min at 4°C. The supernatants (cytosolic fraction) were transferred to a new tube and the mitochondrial pellets were resuspended in cell permeability buffer. After sonication, lysates were resolved on a 15% polyacrylamide gel, and analyzed by immunoblotting using a mouse anti-cytochrome c antibody.

Cell Death, 3-(4,5-dimethylthiazol-2-yl)-2,5-diphenyltetrazolium bromide (MTT) Assay, and Drug Combination Study

To measure cell death, cells were treated with the indicated dose of ABT-737 and cisplatin for 48 h, then stained with annexin-V and propidium iodide (PI) and analyzed using a FACSCanto II flow cytometer (Becton Dickinson, Franklin Lakes, NJ, USA). The effect of treatment on cell proliferation was assessed by the MTT assay. Briefly, 5×10^5 cells per well were treated with either ABT-737 (0–80 μM), cisplatin (0–160 μM), or a combination of both drugs at fixed concentration ratios of 1:0.5, 1:1, and 1:2 (cisplatin:ABT-737). After 48 h, MTT was added at a final concentration of 0.5 mg/mL, and cells were incubated for an additional 2 h at 37°C. Formazan complexes were dissolved in DMSO, and absorbance was measured at 550 nm with a spectrophotometer (Thermo Scientific, Rockford, IL, USA). The effect of combining the therapies was evaluated with a CI previously proposed by Chou-Talalay using CompuSyn software (CompuSyn) [15].

Immunocytochemistry

Cells (5×10^5) were plated in 6-well plates containing a sterilized coverslip. On the following day, cells were fixed with 4% formaldehyde in PBS, incubated in blocking solution containing 5% BSA in PBS, and then incubated with anti-cytochome c, anti-BAK and anti-Bcl-xL antibodies for 16 hours. On the following day, the cells were washed, and

anti-rabbit IgG (Alexa Fluor 488 conjugate) secondary antibodies were added. Mitochondria were stained with MitoTracker Red CMXRos (red). The nuclei were counterstained with DAPI (blue) (1:1000) in PBS and imaged using an LMS 710 confocal microscope (Carl Zeiss, Oberkochen, Germany). Images were acquired using ZEN 2012, Version 8,0,0,273 imaging software (Carl Zeiss, Oberkochen, Germany).

Mouse Imaging

LSL *K-ras* G12D mice were obtained from the NCI mouse repository (http://mouse.ncifcrf.gov/), bred, and genotyped according to the supplier's guidelines. This animal study was approved by our Institutional Animal Care and Use Committee, following the guidelines of the American Association for the Assessment and Accreditation of Laboratory Animal Care. AdCre virus was obtained from the Gene Transfer Vector Core of the University of Iowa (Iowa City, IA, USA). LSL *K-ras* G12D mice inhaled 5×10^7 PFU AdCre virus at eight weeks after birth [16], 24 ± 2 weeks after AdCre particle inhalation, a micro-CT was taken using a small animal eXplore Locus microCT (GE Healthcare, Little Chalfont, UK) under isoflurane anesthesia (45 μm resolution, 80 kV, 450 μA current). The mice were categorized into three groups according to tumor burden (mild, moderate, or severe), and then randomized within the same severity group to receive either vehicle (30% polyethylene glycol, 5% TWEEN 80, and 65% of 5DW solution), ABT-737 (50 mg/kg, i.p., daily), cisplatin (5 mg/kg, i.p., weekly), or a combination of both drugs for two weeks. Treatment response was evaluated by CT image analysis. To measure the area of tumor, first, three representative CT images per mouse were selected at the upper, middle, and lower levels of the lung. Then, the tumor area was quantified in pixels using Adobe Photoshop (Adobe Systems, San Jose, CA) and Paint.Net (dotPDN, LLC, Kirkland, WA) software. Change of tumor area (%) was calculated by $(\text{Pixel}_{\text{before}} - \text{Pixel}_{\text{after}})/\text{Pixel}_{\text{before}} \times 100$ at each level and summated.

IHC

FFPE human NSCLC tissues and mice tissues, sacrificed after the second micro-CT, were analyzed by IHC using the LABS 2 System (Dako, Carpinteria, CA, USA) according to the manufacturer's instructions. Briefly, sections were deparaffinized, rehydrated, immersed in 3% H_2O_2 in methanol solution, and then incubated overnight with primary antibodies against activated caspase-3 in antibody diluent (Dako) at a 1:100 dilution. Sections were incubated for 10 minutes with biotinylated linker and processed using avidin/biotin IHC techniques. 3,3′-Diaminobenzidine (DAB) was used as a chromogen in conjunction with the Liquid DAB Substrate kit (Novacastra, UK). BCL-xL expression was evaluated by a semiquantitative approach [17]. The staining intensity of BCL-xL was evaluated with reference to that of normal appearing adjacent tissues such as bronchial epithelia cells and alveolar macrophages as follows: 0; negative, 1; buff, 2; yellow (similar staining intensity to bronchial epithelial cells), 3; dark brown. The frequency of stained cancer cells was scored as follows: 0; <5%, 1; <25%, 2; <50%, 3; <75%, 4; ~100%. The percentage of positively stained cancer cells and staining intensities were multiplied to generate immunostaining score. The staining scores 0, 1 to 3, 4 to 8, and ≥9 were considered negative, trace, moderate, and strong expression, respectively.

Statistical Analysis

Independent sample *t*-tests were used for univariate analysis of continuous variables. Difference of tumor area change among groups was analyzed by Mann–Whitney *U* test. Predictive factors for disease-free survival (DFS) and overall survival (OS) were calculated using the

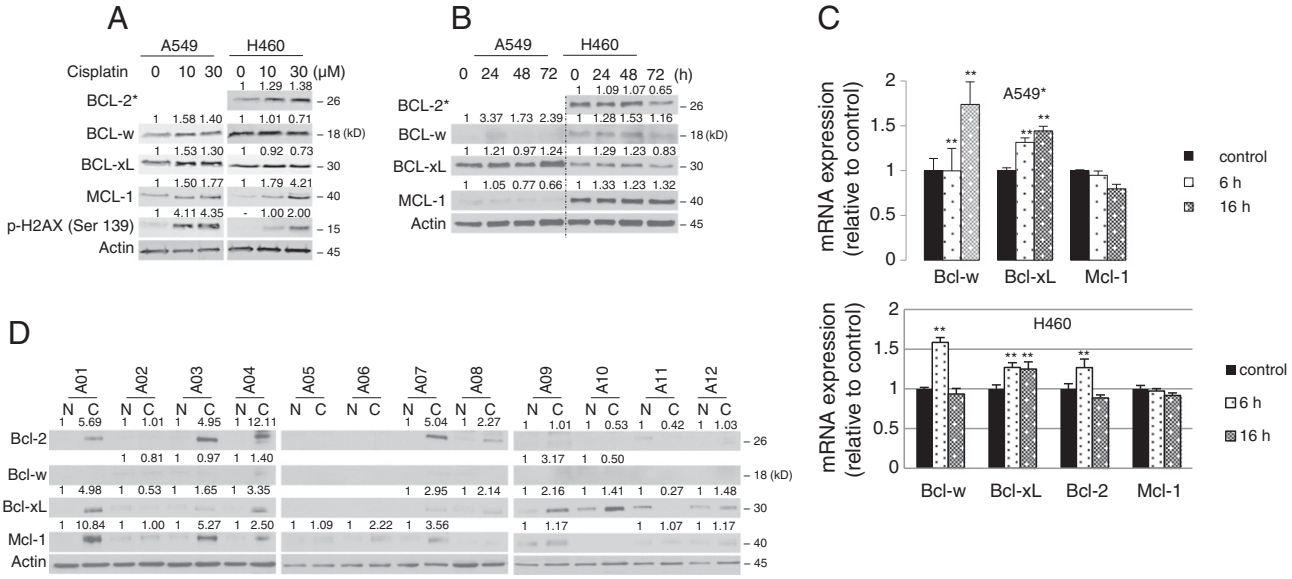

Figure 1. Cisplatin induces overexpression of anti-apoptotic proteins. (A) A549 and H460 cells were treated with 10 and 30 μM of cisplatin for 24 h and expression of anti-apoptotic molecules was evaluated by immunoblotting. (B) A549 and H460 cells were treated with 3 μM of cisplatin for 1, 2, 3 days and expression of anti-apoptotic molecules was evaluated by immunoblotting. (C) A549 and H460 cells were treated with cisplatin for 6 and 16 h and mRNA expression of anti-apoptotic molecules was evaluated by real time PCR. (D) Expression of anti-apoptotic molecules was evaluated by immunoblotting using a set of cancer enriched and normal appearing adjacent lung tissue lysates from 12 NSCLC patients. All experiments were repeated more than 3 times and the representative figure was shown. Actin was used as a loading control and p-H2AX (Ser139) were used as a marker for cisplatin mediated DNA damage. IPO8 was used as an internal control for RT-PCR. *A549 cells do not express BCL-2 (http://www.proteinatlas.org/ENSG00000171791-BCL2/cell/CAB000003). ***P*-value was less than 0.05 when compared with control (independent sample *t*-test).

Kaplan–Meier estimator. SPSS software (v. 18; SPSS, IL, USA) was used for statistical analysis. All statistical analyses were two-tailed and *p*-values of less than 0.05 were interpreted to indicate statistical significance.

Results

Increased Expression of Anti-Apoptotic Proteins After Cisplatin Treatment

Alterations in apoptotic pathway by cisplatin induced DNA damage responses are frequently observed after treatment of cisplatin and have been estimated to be a major cause of treatment failure [18,19]. To confirm this, NSCLC cells were treated with cisplatin and expression of anti-apoptotic protein was evaluated by immunoblotting using phosphorylation of H2AX at Ser139 as a cisplatin-induced DNA double strand breakage marker. There was dose and time dependent overexpression of BCL-2 family member proteins after cisplatin treatment (Figure 1, *A* and *B*). To determine the increase in anti-apoptotic molecules at the transcriptional level after cisplatin treatment, A549 and H460 cells were treated with cisplatin for 6 and 16 h and mRNA expression of anti-apoptotic molecules was evaluated by real time PCR (RT-PCR). The mRNA levels of the anti-apoptotic molecules increased and reached a peak at 6 h after treatment after which they decreased. Among them, *BCL-w* mRNA levels increased more than those of the other molecules did (Figure 1*C*). Taken together, cisplatin induced overexpression of BCL-2 family member of anti-apoptotic protein occurred at the transcriptional level in part.

Anti-Apoptotic Proteins are Frequently Overexpressed in NSCLC

To evaluate overexpression of anti-apoptotic proteins in NSCLC, immunoblotting was performed using a set of paired cancer enriched and normal appearing adjacent tissue lysates from 12 NSCLC patients (Table 1 and Figure 1*D*). Among the 12 pairs, eight cases (66.7%) showed increased expression of BCL-xL in the lung cancer enriched tissue lysates when compared in the lysate of adjacent normal appearing lung tissues, followed by BCL-2 and MCL-1 overexpression in five pairs (41.7%) respectively. BCL-w showed weak expression in the two cases, which did not differ between the cancer-enriched and adjacent tissue lysates, and overexpression in the cancer lysate in one case.

Because BCL-xL was the one, which was specifically expressed in cancer-enriched tissue lysates with high frequency, its clinical implication was evaluated in 117 FFPE NSCLC tissues by IHC. The demographic characteristics of the 117 NSCLC cases were described in the Table 2. BCL-xL was mainly expressed in the cytoplasm of lung cancer cells (Figure 2*A*). A total of 88 (75.2%) NSCLC cases showed positive BCL-xL expression, which was comparable to the results of immunoblotting (Figure 2*B*). Then the clinical outcome of the study cases was analyzed according to the expression of BCL-xL. Although the difference of DFS and OS did not reach statistical significance between negative/trace vs. positive expression group, there were clear separation of survival curve between groups (Figure 2*C*). These findings are also observed in a subset analysis using the cases who underwent adjuvant chemotherapy after curative resection (data not shown). Taken together, anti-apoptotic proteins were specifically overexpressed in NSCLC cancer tissues and overexpression of BCL-xL was most frequent.

Table 1. Demographic Characteristics of the NSCLC Cases Used for Immunoblotting

Random No.	Gender	Age	Histology	Differentiation	Smoking	TNM	Stage
A01	F	76	Adeno	n.s*	Never smoker	T3N0M0	IIB
A02	F	48	Adeno	acinar type	Never smoker	T1aN2M0	IIIA
A03	M	75	Adeno	solid predominant	Ex-smoker	T2aN0M0	IB
A04	F	75	Adeno	papillary predominant	Never smoker	T1bN0M0	IA
A05	M	67	Squamous	n.s*	Never smoker	T2aN0M0	IB
A06	M	68	Squamous	moderate	Current smoker	T2aN1M0	IIA
A07	M	65	Squamous	poorly	Ex-smoker	T2aN0M0	IB
A08	M	62	Adeno	micropapillary predominant pattern	Ex-smoker	T2aN1M0	IIA
A09	M	59	Adeno	micropapillary predominant with mucin formation	Current smoker	T2aN2M0	IIIA
A10	M	71	Adeno	acinar predominant	Current smoker	T1bN2M0	IIIA
A11	M	66	Squamous	moderate	Ex-smoker	T2bN2M0	IIIA
A12	F	74	Adeno	acinar predominant	Never smoker	T2aN0M0	IB

n.s; not specified.

Table 2. Clinical and Pathological Characteristics of 117 NSCLC Cases Used for IHC Analysis

Clinical Characteristics	Cytoplasmic Expression (n = 117)		
	Negative/Trace (n = 31)	Positive (n = 86)	*P*-value
Gender			
Male	25	62	0.350
Female	6	24	
Smoking status			0.811
Never smokers	6	23	
Ever smokers	22	55	
Maximal diameter of tumor (㎝)	4.2 ± 1.94	4.2 ± 2.09	0.976
pStage			0.708
I	12	26	
II	7	20	
III	12	38	
IV	0	2	
Pathologic diagnosis			0.237
Adenocarcinoma	12	47	
Squamous cell carcinoma	19	38	
Others	0	1	

Smoking status of 11 cases was unknown.

STAT3 Mediates Cisplatin-Induced Elevation of Anti-Apoptotic Molecules

To identify the underlying mechanism that induces overexpression of the antiapoptotic protein family, NSCLC cell lines, A549 and H460, were treated with various doses and times of cisplatin and the phosphorylation of JNK and SRC was evaluated. After cisplatin treatment, phosphorylation of JNK and SRC increased, reaching a peak after about 24 h, followed by a decrease (Figure 3, *A*–*C*). To determine whether the elevation of antiapoptotic proteins was mediated by JNK1, A549 and H460 cells were transfected with constitutive active form of JNK1 (MKK7-JNK1) and kinase dead form (MKK7-JNK1(APF)). These cells were also treated with the JNK1-specific activator, anisomycin, and evaluated using the same methods (Figure 3*D*). No differences were noted in the expression of antiapoptotic proteins between constitutive active and kinase dead transfected cells. After anisomycin treatment, the expression of BCL-xL and other anti-apoptotic molecules decreased, suggesting that the elevation of the anti-apoptotic molecules was not mediated by JNK. Further, to confirm whether the increased expression of anti-apoptotic protein is mediated by STAT3 activation, the effect of SRC phosphorylation was evaluated by immunoblotting. The phosphorylation of SRC was relayed to phosphorylation of STAT3 through JAK2 with the passage of time (Figure 3*E*). The dominant negative form of STAT3, EF.STAT3DN, was then transfected, and the effect on expression of BCL-xL and other anti-apoptotic molecules was evaluated by immunoblotting.

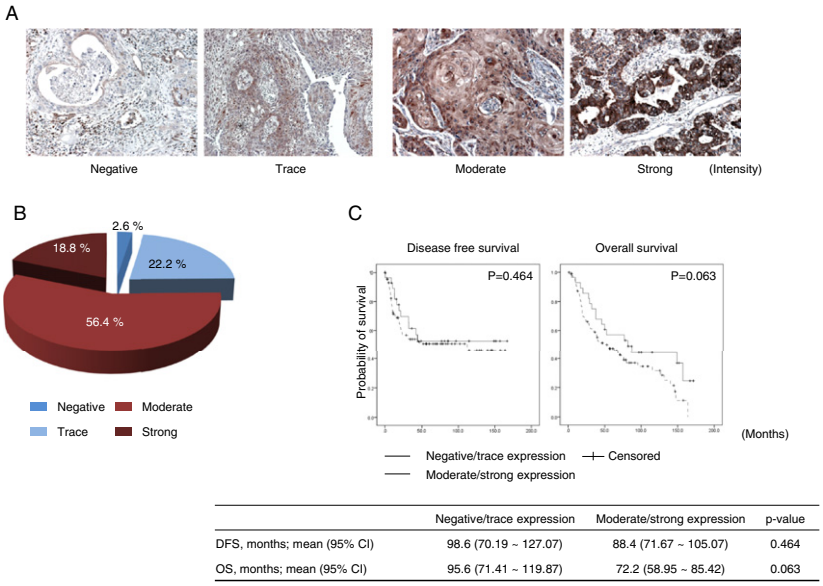

	Negative/trace expression	Moderate/strong expression	p-value
DFS, months; mean (95% CI)	98.6 (70.19 ~ 127.07)	88.4 (71.67 ~ 105.07)	0.464
OS, months; mean (95% CI)	95.6 (71.41 ~ 119.87)	72.2 (58.95 ~ 85.42)	0.063

Figure 2. BCL-xL is frequently overexpressed in NSCLC. (A) Expression of BCL-xL in FFPE NSCLC tissues was analyzed by IHC. BCL-xL expression was evaluated by a semiquantitative approach, and then staining scores 0, 1 to 3, 4 to 8 and ≥9 were considered negative, trace, moderate, and strong expression, respectively. The expression score was 4 or more, it was defined as positive BCL-xL expression. (B) BCL-xL expression was analyzed by IHC in the 117 NSCLC cases. A total of 88 (75.2%) NSCLC cases showed positive BCL-xL expression. (C) DFS and OS was analyzed according to the expression of BCL-xL in the 117 NSCLC cases using the Kaplan–Meier estimator. *P*-value was obtained by Log-rank test.

Anti-apoptotic protein levels decreased after transfection with EF.STAT3DN. When the EF.STAT3DN transfected A549 and H1299 cells were treated with cisplatin, the increase in the levels of the anti-apoptotic molecules was blunted (Figure 3*F*). To determine the effect on the expression of BCL-xL by cisplatin mediated activation of SRC pathway, additional experiment was performed using SRC inhibitor, dasatinib (Figure 3*G*). Pretreatment of dasatinib suppressed elevation of pSTAT3 by cisplatin, leading inhibition of BCL-xL expression. These findings suggest that the increase in BCL-*2* protein family is caused by cisplatin-mediated STAT3 activation.

Cisplatin Potentiates Inherent Characteristics of BH3 Mimetics

ABT-737, a small-molecule BH3 mimetic, disrupts the BCL-2/BAK complex and BAK-dependent activation of the intrinsic apoptotic pathway [20]. First, to identify the inherent characteristic of the ABT-737, A549 cells were treated with ABT-737, and subcellular fractionation was performed. Cytochrome *c* was released from the mitochondria and accumulated in the cytosol after ABT-737 treatment in a dose- and time-dependent manner (Figure 4*A*). Confocal microscopy revealed that ABT-737 displaced BCL-xL from mitochondria and induced aggregation BAK signal and co-localization at mitochondria. It also showed that ABT-737 displaced cytochrome c from mitochondria into cytoplasm, and this effect was not influenced when combined with cisplatin treatment (Figure 4*B*). To clarify the effect of combination on cytochrome c release, immunoblotting on subcellular fraction was performed (Figure 4*C*). Displacement of cytochrome c from mitochondrial fraction to cytoplasm was more evident by combination treatment in the immunoblotting. Taken together, cisplatin treatment did not disturb inherent characteristic of BH3 mimetics but potentiated.

Synergy of Cisplatin and BH3 Mimetics

The effect of this combination was further evaluated whether these molecular findings lead to synergistic effect on cell death using immunoblotting, flow cytometer, and tetrazolium-based colorimetric (MTT) assay and CI was obtained by the method proposed by Chou-Talalay [15]. As demonstrated by immunoblotting and flow cytometric analysis of cell death, the combination of cisplatin and ABT-737 potentiated the cytotoxic effects of cisplatin (Figure 5, *A* and *B*). To determine the synergistic effect of both drugs by cell death assay, A549 and H460 cells were treated with 1:1 fixed ratios of cisplatin to ABT-737 for 48 h, and cell death was measured by flow cytometer by the Annexin V-PI staining. Statistically significant increment in cell death occurred in the combination treatment group (Figure 5*C*), and CI was obtained by the Chou-Talalay method (Supplementary Figure S1). To further determine whether the increase in cell death was the synergistic effect of the cisplatin and ABT-737 at various concentration and to find out optimal combination condition, both drugs were combined at fixed dose ratios and the MTT assay was performed. The CI–F(a) and Dose–F(a) curves generated from the MTT assay results demonstrated a strong synergism in A549 cells and a synergism in H460 cells when combination therapy was used (Figure 5, *D* and *E*). To further confirm the synergistic effect of both drugs, additional experiments were performed using five different NSCLC cell lines, H1299, H358, H2009, H1703, and H596. Strong synergism was observed in H596 cells and synergism was shown in other NSCLC cell lines (Supplementary Figure S2).

Combination Effect of Cisplatin and BH3 Mimetics in Animal Model

To validate the effect of combination treatment in vivo, 34 ± 2 week-old mice that had been infected with AdCre by inhalation were randomized and treated with vehicle, cisplatin (5 mg/kg, i.p., weekly), ABT-737 (50 mg/kg, i.p., daily), or a combination of both drugs (Figure 6*A*). Response was measured by micro-CT (Figure 6*B*). Statistically significant reductions in tumor size occurred in the combination treatment group (P = .029; Mann–Whitney U test)

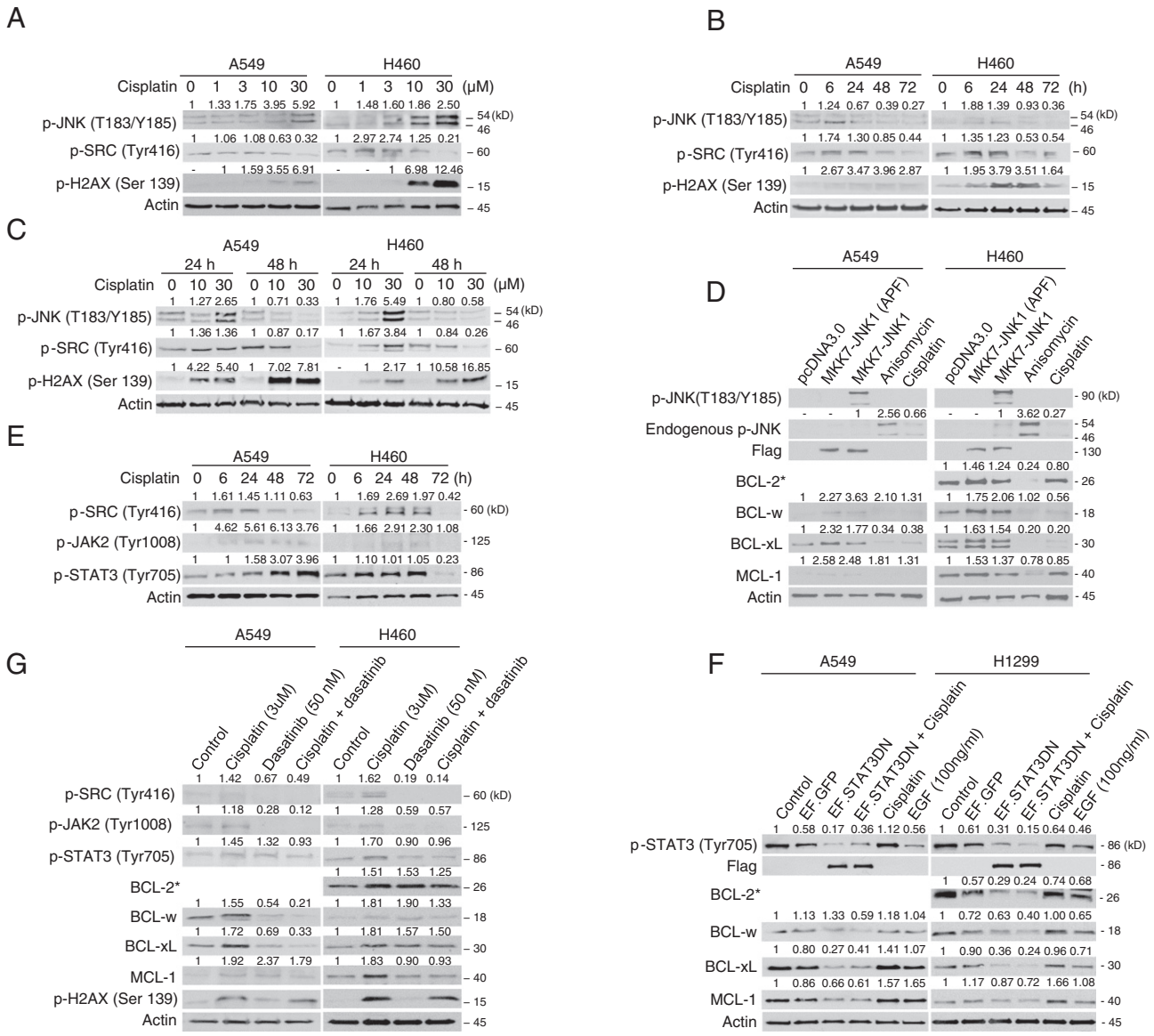

Figure 3. STAT3 mediates cisplatin-induced elevation of anti-apoptotic molecules. (A) A549 and H460 cells were treated with indicated dose of cisplatin for 16 h and the phosphorylation of JNK and SRC was evaluated by immunoblotting. (B) A549 and H460 cells were treated with 3 μM of cisplatin for indicated times and phosphorylation of JNK and SRC was evaluated by immunoblotting. (C) A549 and H460 cells were treated with indicated doses and times of cisplatin and evaluated using the same methods. (D) A549 and H460 cells were transfected with constitutive active form of JNK (MKK-JNK1), kinase dead form (MKK-JNK1(APF)) and treated with JNK1-specific activator, anisomycin. Phosphorylation of JNK and expression of anti-apoptotic molecules was evaluated by immunoblotting. (E) A549 and H460 cells were treated with cisplatin for indicated times and phosphorylation of SRC, JAK2 and STAT3 was evaluated by immunoblotting. (F) A549 and H1299 cells were transfected with dominant negative form of STAT3, EF.STAT3DN, and treated with or without cisplatin. Expression of anti-apoptotic molecules was evaluated by immunoblotting. (G) A549 and H460 cells were treated with 3 μM of cisplatin and/or 50 nM of SRC inhibitor, dasatinib, for 16 h. Expression of p-SRC, pSTAT3 and BCL-xL were evaluated by immunoblotting. Actin was used as a loading control and p-H2AX (Ser139) were used as a marker for cisplatin mediated DNA damage. *A549 cells do not express BCL-2 (http://www.proteinatlas.org/ENSG00000171791-BCL2/cell/CAB000003).

(Figure 6*C*). Lungs were harvested after imaging and analyzed by H&E and immunohistochemistry (Figure 6, *D* and *E*). Together with morphologic changes in the combination treatment group, showing shrunken cytoplasm and condensed nuclei, expression of activated caspase-3 was more frequently detected in the combination groups. In summary, a significant tumor reduction was observed after two weeks in LSL *K-ras* G12D mice following combined treatment with cisplatin and ABT-737 compared to treatment with vehicle or either agent alone. To determine the toxicity of ABT-737, mouse body weight was measured daily. Weight loss in the combination group was not significantly different compared to the monotherapy groups; combination treatment with cisplatin and ABT-737 is thus a tolerable treatment (Figure 6, *F* and *G*).

Because p53 plays a major role in the initiation of the apoptotic pathway in DNA damaged cells, additional experiments were performed using LSL K-ras G12D:p53$^{fl/fl}$ mice (Supplementary Figure S3). The median survival of this model is about 14 weeks after AdCre inhalation and tumors show aggressive phenotypes with high

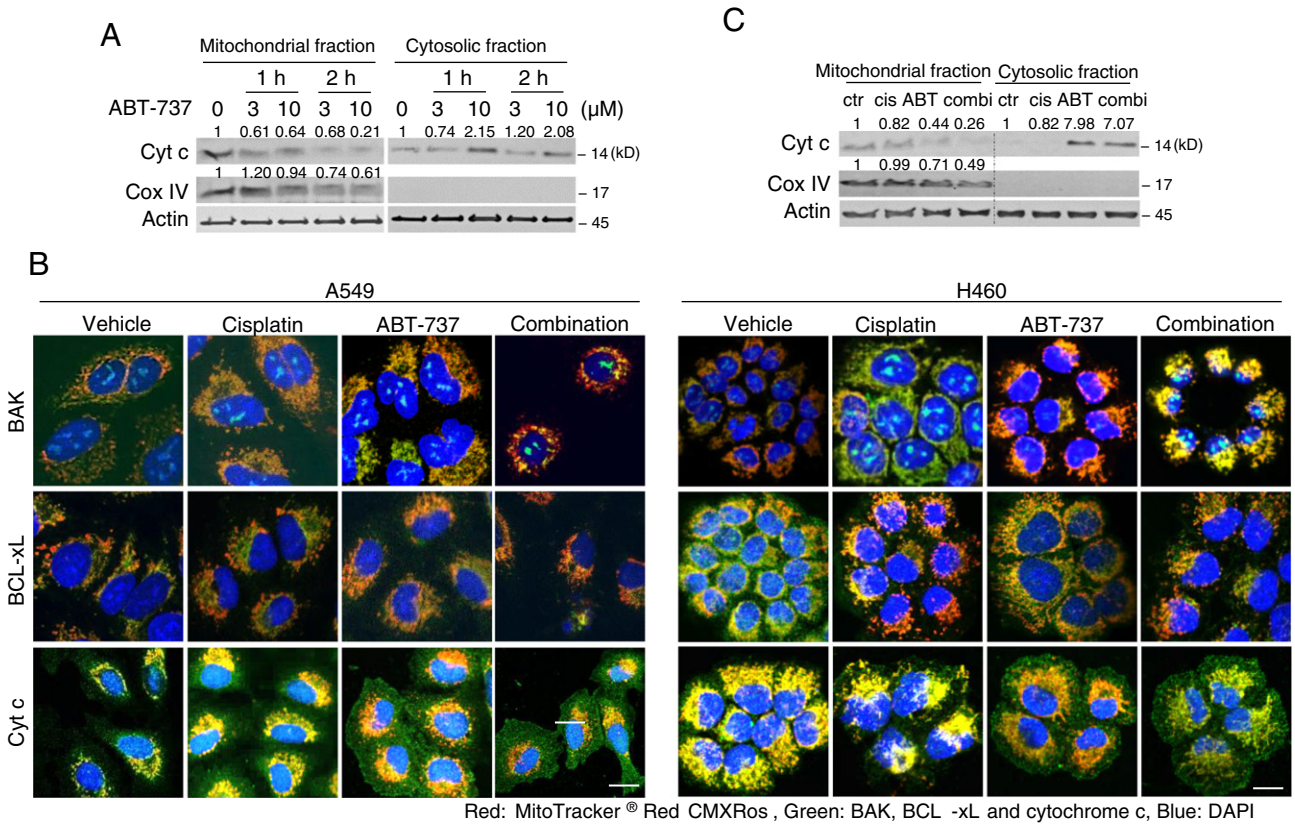

Figure 4. BH3 mimetics bypass cisplatin-induced elevation of anti-apoptotic molecules. (A) A549 and H460 cells were treated with indicated dose of cisplatin for 1 or 2 h and subcellular fractionation was performed. (B) Immunofluorescence staining of BAK, BCL-xL and cytochrome c. Treatment with ABT-737 displaced BCL-xL from mitochondria and induced co-localization of BAK with MitoTracker, a mitochondrial marker. Release of the cytochrome c into the cytoplasm after ABT-737 treatment was visualized. Mitochondria were stained with MitoTracker Red CMXRos (red), and BAK, BCL-xL and cytochrome c were visualized with an Alexa-488 conjugated secondary antibody (green). The nuclei were counterstained with DAPI (blue) (magnification; ×630, white scale bar; 10 μm) (C) A549 cells were treated with cisplatin, ABT-737, or a combination of both drugs and subcellular fractionation was performed. All experiments were repeated more than 3 times and the representative figure was shown. Actin was used as a loading control and Cox IV was used for a marker for subcellular fraction. ctr: control, cis: cisplatin, ABT: ABT-737, combi: combination.

multiplicity [21]. After 12 ± 2 weeks after AdCre inhalation (20 ± 2 week-old), the mice were treated and evaluated in the same manner as in LSL *K-ras* G12D mice. Although it did not reach statistical significance, combination treatment group showed reduced tumor burden when compared with cisplatin or ABT-737 monotherapy group, which is consistent to the findings in LSL K-ras G12D mice model. Morphologic changes, which indicates apoptosis, were frequently observed and expression of activated caspase-3 was statistically higher in the lung of combination group, suggesting that this combination is effective in the cancer with p53 loss.

Discussion

Targeted treatment strategies focusing on the genetic variation of a specific gene are of limited use for the treatment of a subset of lung cancer, in which druggable driver mutation was not identified, suggesting that new strategies aiming the common elements of cancer are required. One of the hallmarks of cancer is its ability to resist cell death using various mechanisms to circumvent the apoptotic pathway [6]. Besides loss of function of TP53 tumor suppressor, which induces apoptosis of critically damaged cells [22], decreased function of proapoptotic factors (BAX, BIM, and PUMA), and elevation of antiapoptotic regulators (BCL-2, BCL-xL, and BCL-w) are frequently observed [2]. The aberrant regulation of the apoptotic pathway is not only an inherent characteristic of the cancer cells, but it can be induced by drug treatment and influences drug sensitivity.

Platinum-based chemotherapeutic agents have been extensively used for the treatment of solid tumors, and the resistance mechanisms against these agents have been studied widely [2,23]. However, reports on the effects of apoptosis protein expression by cisplatin treatment are limited. Cisplatin-mediated increase in the activity of MAPK family members was clearly observed in a dose- and time-dependent manner in various in vitro and in vivo experimental settings. Studies have shown varying effects of increased ERK1, JNK, and STAT3 activities on cisplatin sensitivity. A recent meta-analysis concluded that, depending on the experimental setting, increased JNK activity can either increase [24–27] or decrease sensitivity [28,29] to cisplatin treatment. However, previous studies were based mostly on cell culture assays and the results from in vivo systems are limited, indicating that animal studies are required to provide a conclusive relationship between JNK activity and cisplatin. In our study, by using lung cancer cell lines, the JNK inhibitor SP600125 was not able to induce growth inhibition in the MTT assay even when using concentrations of up to 80 μM but it potentiated the cytotoxic effect of cisplatin when both agents were combined (data not shown). With these findings, a negligible effect on the expression of anti-apoptotic proteins suggests that the activation of JNK might not

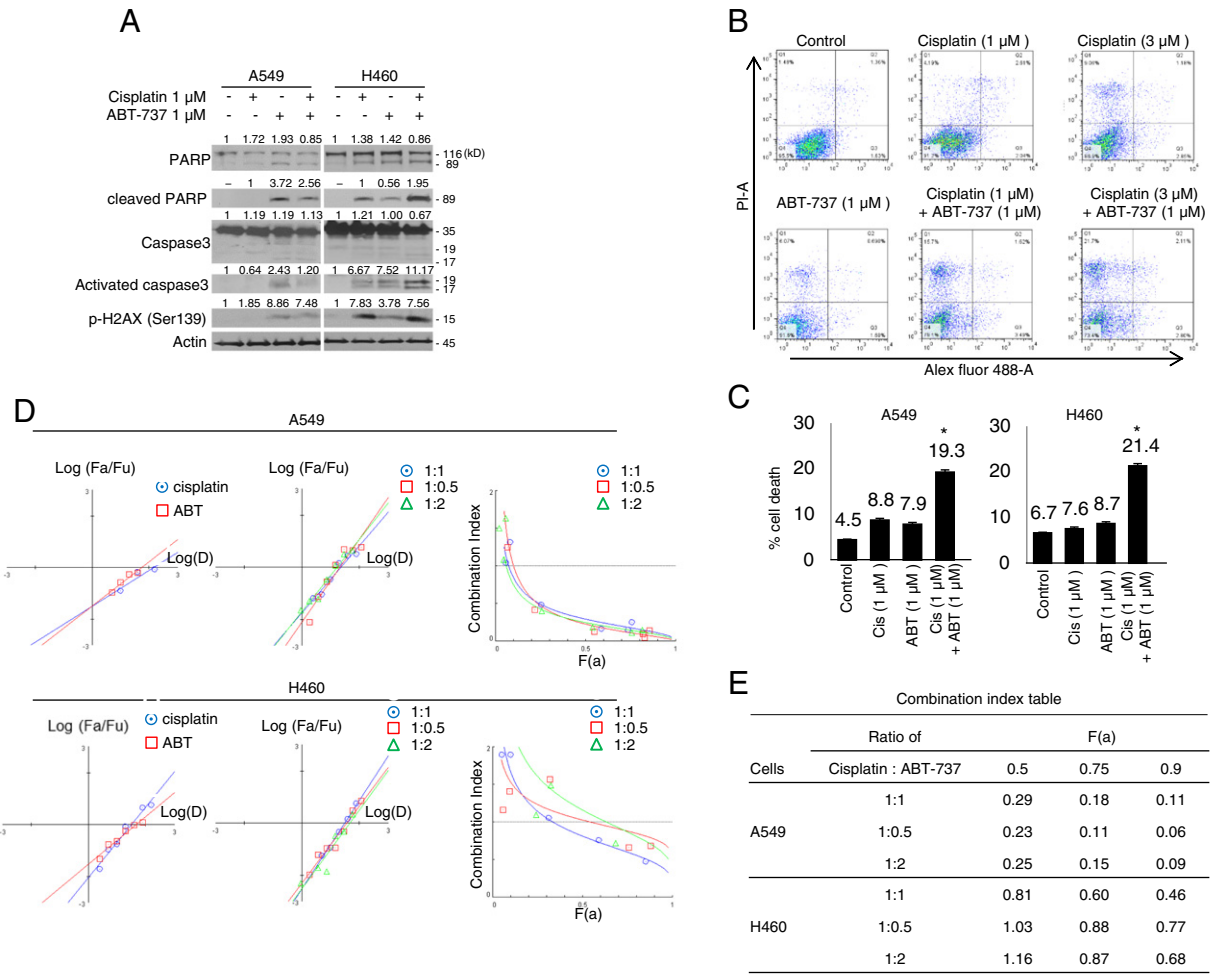

Figure 5. Synergy of cisplatin and BH3 mimetics. (A) A549 and H460 cells were treated with cisplatin with or without ABT-737 for 48 h and cell death was evaluated by immunoblotting. (B) A549 cells were treated with cisplatin with or without ABT-737 for 48 h and cell death was evaluated using flow cytometry after Annexin V and PI staining. (C) The histogram denoting % cell death for A549 and H460 cells treated with 1:1 fixed ratios of cisplatin to ABT-737 for 48 h. Cell death was measured by flow cytometer by the Annexin V-PI staining. (D) F(a)-dose and F(a)-CI curve for A549 and H460 cells treated with cisplatin and ABT-737. A549 and H460 cells were treated with different fixed ratios of cisplatin to ABT-737 (1:1, 1:0.5 and 1:2) for 48 h, and cell viability was determined using the MTT assay. (E) Combination index was estimated by CompuSyn software and combination index at indicated fraction affected (F(a)) was shown. Actin was used as a loading control and p-H2AX (Ser139) were used as a marker for cisplatin mediated DNA damage. All experiments were repeated more than 3 times and the representative figure was shown. F(a): fraction affected. Cis: cisplatin, ABT: ABT-737.

play a major role in the cisplatin resistance. There are in vitro evidences indicating that cisplatin affects the gene expression of ubiquitin-proteasome system and inhibits activity of proteasome [30,31]. In the experiments with bortezomib, 20S proteasome inhibition broadly influences on the expression of BCL-2 family protein [32,33]. These reports suggest that the inhibition of the proteasome pathway by cisplatin might be another of increased expression of BCL-xL, but requires further studies to connect cisplatin treatment and BCL-2 family protein expression. STAT3 is one of key downstream mediators of activated EGFR and is activated by various signals such as interferon, IL-5, and IL-6. It plays multiple roles in tumorigenesis involving inflammation, stem cells, and pre-metastatic niche [34]. A meta-analysis by Xu et al. showed that high STAT3 or pSTAT3 expression is a strong predictor of poor prognosis in NSCLC patients [35]. Although the underlying mechanism that relates over-expression of STAT3 and poor clinical outcome is not well established, our in vitro experiments suggested that it might be related to the expression of anti-apoptotic proteins. Further prospective translational studies may be warranted to substantiate this.

The advantages of combination chemotherapy include the emergence of synergistic interaction effects, the ability to overcome of multidrug resistant clones, and the reduction of the drug dose with a concomitant diminished toxicity to healthy tissues [36,37]. The general principles of cancer drug combinations are to (1) use drugs with non-overlapping toxicities, (2) combine agents with different mechanisms of action and minimal cross-resistance, (3) preferentially use drugs with proven activity as single drugs, and (4) administer the combination at early-stage disease and at a schedule with a minimal treatment-free period between cycles, but allowing the recovery of sensitive target tissues. Based on this classical principle, co-treatment with cisplatin and BH3 mimetics would be an optimal combination regimen for the treatment of lung cancer.

Based on these findings, application of BH3 mimetics for the treatment of lung cancer seems to be promising; however, the

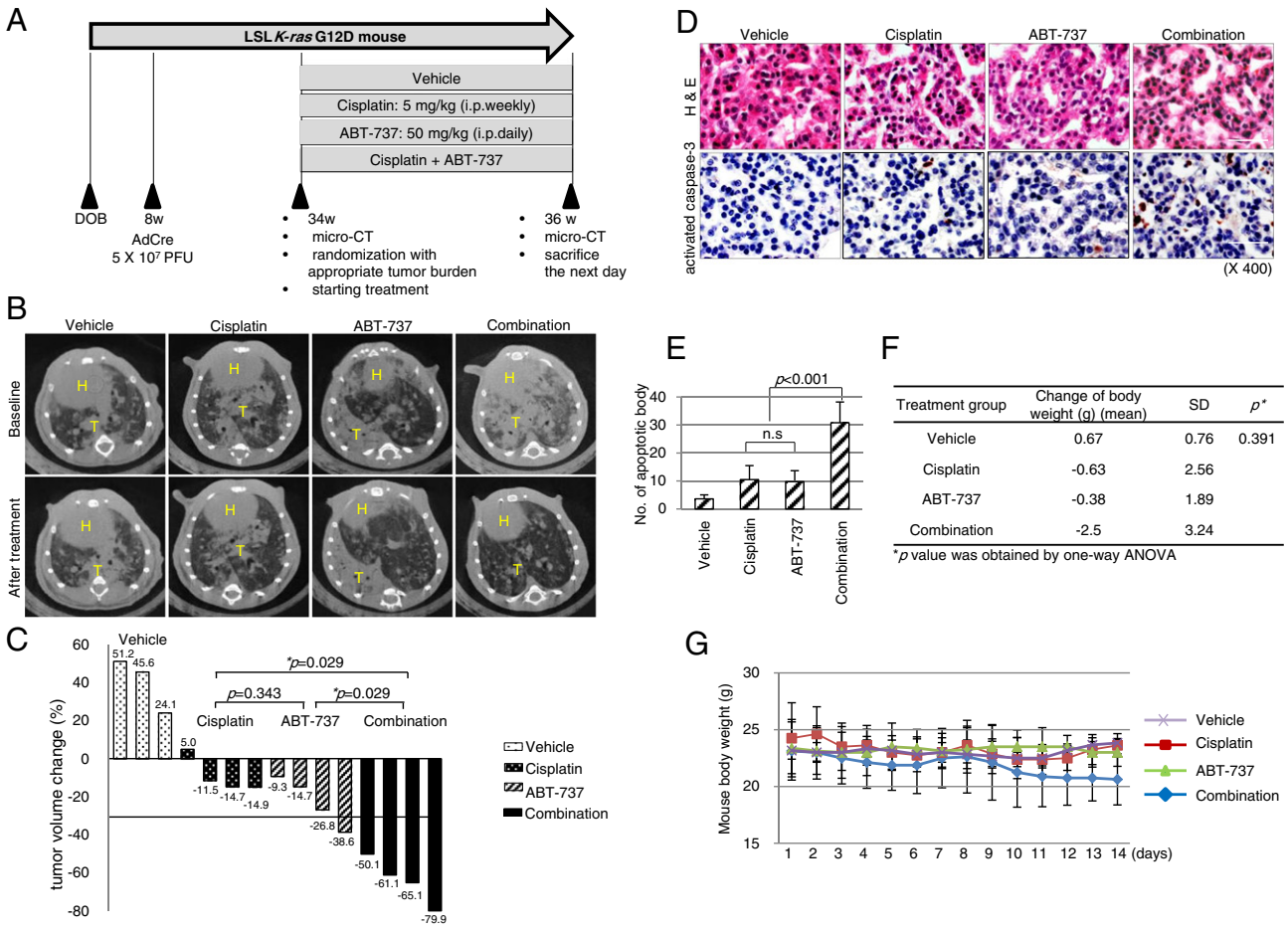

Figure 6. Combination effect of cisplatin and ABT-737 in a *K-ras* mutant lung cancer mouse model. (A) Treatment schedule of the LSL *K-ras* G12D mouse study. Eight-week old heterozygote of LSL *K-ras* G12D mice were inhaled with 5×10^7 PFU AdenoCre virus. At 34 ± 2 weeks, the mice were underwent microCT and were randomized according to lung tumor severity, and then treated with vehicle, cisplatin, ABT-737, or combination of both drugs for two weeks. (B) The treatment response was evaluated by comparing microCT images taken before and after treatment. H; heart, T; tumor. (C) Waterfall plot showing tumor response after two weeks of treatment. Each column represents one individual mouse. *P*-value was obtained by Mann–Whitney *U* test. (D) H&E staining and activated caspase-3 immunohistochemical analysis of the lungs of treated mice. For immunohistochemistry, DAB was used as a chromogene. (magnification; ×400, white scale bar; 50 μm). (E) The number of the apoptotic body per high power field (×400) was presented as histogram. The apoptotic body was counted at 8 fields and the number was compared by Student *t*-test. n.s.: not significant. (F and G) Change of mouse body weight during treatment was shown. The change of before and after 2 weeks treatment were compared by one-way ANOVA.

outcome of clinical trials with BH3 mimetics alone for cancer treatment was modest [38]. It may be attribute to that ABT-737 was not easy to be administered up to the maximum doses because of toxicity. Because survival of platelet is dependent to BCL-xL, thrombocytopenia is one of major adverse effects of the ABT-737 treatment [39]. In this study, the hematologic profile was evaluated in a subset of mice at the end of treatment (Supplementary Table 1). Significant thrombocytopenia was observed in the mice treated with the cisplatin and combination regimen. This suggests that risk of bleeding events could be further increased in the combination regimen containing cisplatin, and that further studies on the dosing and treatment schedules are required. Because of concerns about hematologic toxicities, there are attempts to improve pharmaceutical formulation such as nanoencapsulation of ABT-737. These strategies expect to reduce the toxicity and enhance efficacy of combination treatment with ABT-737 [40]. In addition, selective, oral BCL-2 inhibitor sparing platelets, ABT-199, was developed and studied in several ongoing trials with single or combination regimens [41].

Another useful method for evaluating the efficacy of this new regimen is to determine if the treatment prolongs survival. For this purpose, a few mice treated with the combination regimen have been monitored for their overall survival. Because of the limited number of the mice, the full statistics could not be obtained. The median survival duration of combination treatment group was 6.3 months from treatment and this indicates that additional methods to test the efficacy of the combination treatment, such as observation of progression free survival with repeated imaging, may be required.

In conclusion, we investigated the changes in the levels of anti-apoptotic molecules mediated by cisplatin-induced STAT3 activation in depth. Additionally, we found that co-treatment with BH3 mimetics could help to bypass cisplatin resistance. The modulation of the apoptotic pathway, which determines the cell fate of damaged cells, with BH3 mimetics would be an effective way to overcome the barriers in NSCLC treatment caused by intratumoral heterogeneity.

Supplementary data to this article can be found online at http://dx.doi.org/10.1016/j.neo.2017.02.008.

Funding Information

This study was supported by Basic Science Research Program through the National Research Foundation of Korea (NRF) funded by the Ministry of Science, ICT & Future Planning (grant No. NRF-2015R1C1A1A02037675) given to EY Kim.

References

[1] Torre LA, Bray F, Siegel RL, Ferlay J, Lortet-Tieulent J, and Jemal A (2015). Global cancer statistics, 2012. *CA Cancer J Clin* **65**, 87–108.

[2] Galluzzi L, Senovilla L, Vitale I, Michels J, Martins I, Kepp O, Castedo M, and Kroemer G (2012). Molecular mechanisms of cisplatin resistance. *Oncogene* **31**, 1869–1883.

[3] Williams J, Lucas PC, Griffith KA, Choi M, Fogoros S, Hu YY, and Liu JR (2005). Expression of Bcl-xL in ovarian carcinoma is associated with chemoresistance and recurrent disease. *Gynecol Oncol* **96**, 287–295.

[4] Michaud WA, Nichols AC, Mroz EA, Faquin WC, Clark JR, Begum S, Westra WH, Wada H, Busse PM, and Ellisen LW, et al (2009). Bcl-2 blocks cisplatin-induced apoptosis and predicts poor outcome following chemoradiation treatment in advanced oropharyngeal squamous cell carcinoma. *Clin Cancer Res* **15**, 1645–1654.

[5] Kim EY, Kim A, Kim SK, and Chang YS (2015). AZD6244 inhibits cisplatin-induced ERK1/2 activation and potentiates cisplatin-associated cytotoxicity in K-ras G12D preclinical models. *Cancer Lett* **358**, 85–91.

[6] Hanahan D and Weinberg RA (2011). Hallmarks of cancer: the next generation. *Cell* **144**, 646–674.

[7] Strasser A, Cory S, and Adams JM (2011). Deciphering the rules of programmed cell death to improve therapy of cancer and other diseases. *EMBO J* **30**, 3667–3683.

[8] Lessene G, Czabotar PE, and Colman PM (2008). BCL-2 family antagonists for cancer therapy. *Nat Rev Drug Discov* **7**, 989–1000.

[9] Ni Chonghaile T and Letai A (2008). Mimicking the BH3 domain to kill cancer cells. *Oncogene* **27**(Suppl. 1), S149–S157.

[10] Park D, Magis AT, Li R, Owonikoko TK, Sica GL, Sun SY, Ramalingam SS, Khuri FR, Curran WJ, and Deng X (2013). Novel small-molecule inhibitors of Bcl-XL to treat lung cancer. *Cancer Res* **73**, 5485–5496.

[11] Oltersdorf T, Elmore SW, Shoemaker AR, Armstrong RC, Augeri DJ, Belli BA, Bruncko M, Deckwerth TL, Dinges J, and Hajduk PJ, et al (2005). An inhibitor of Bcl-2 family proteins induces regression of solid tumours. *Nature* **435**, 677–681.

[12] Lee EF, Czabotar PE, Smith BJ, Deshayes K, Zobel K, Colman PM, and Fairlie WD (2007). Crystal structure of ABT-737 complexed with Bcl-xL: implications for selectivity of antagonists of the Bcl-2 family. *Cell Death Differ* **14**, 1711–1713.

[13] Kim A, Kim EY, Cho EN, Kim HJ, Kim SK, Chang J, Ahn CM, and Chang YS (2013). Notch1 destabilizes the adherens junction complex through upregulation of the Snail family of E-cadherin repressors in non-small cell lung cancer. *Oncol Rep* **30**, 1423–1429.

[14] Souers AJ, Leverson JD, Boghaert ER, Ackler SL, Catron ND, Chen J, Dayton BD, Ding H, Enschede SH, and Fairbrother WJ, et al (2013). ABT-199, a potent and selective BCL-2 inhibitor, achieves antitumor activity while sparing platelets. *Nat Med* **19**, 202–208.

[15] Chou TC (2006). Theoretical basis, experimental design, and computerized simulation of synergism and antagonism in drug combination studies. *Pharmacol Rev* **58**, 621–681.

[16] Wang J, Zhou JY, and Wu GS (2011). Bim protein degradation contributes to cisplatin resistance. *J Biol Chem* **286**, 22384–22392.

[17] Zhang Y, Zhang Y, Yun H, Lai R, and Su M (2014). Correlation of STAT1 with apoptosis and cell-cycle markers in esophageal squamous cell carcinoma. *PLoS One* **9**, e113928.

[18] Pan B, Yao KS, Monia BP, Dean NM, McKay RA, Hamilton TC, and O'Dwyer PJ (2002). Reversal of cisplatin resistance in human ovarian cancer cell lines by a c-jun antisense oligodeoxynucleotide (ISIS 10582): evidence for the role of transcription factor overexpression in determining resistant phenotype. *Biochem Pharmacol* **63**, 1699–1707.

[19] Potapova O, Haghighi A, Bost F, Liu C, Birrer MJ, Gjerset R, and Mercola D (1997). The Jun kinase/stress-activated protein kinase pathway functions to regulate DNA repair and inhibition of the pathway sensitizes tumor cells to cisplatin. *J Biol Chem* **272**, 14041–14044.

[20] Konopleva M, Contractor R, Tsao T, Samudio I, Ruvolo PP, Kitada S, Deng X, Zhai D, Shi YX, and Sneed T, et al (2006). Mechanisms of apoptosis sensitivity and resistance to the BH3 mimetic ABT-737 in acute myeloid leukemia. *Cancer Cell* **10**, 375–388.

[21] Ji H, Ramsey MR, Hayes DN, Fan C, McNamara K, Kozlowski P, Torrice C, Wu MC, Shimamura T, and Perera SA, et al (2007). LKB1 modulates lung cancer differentiation and metastasis. *Nature* **448**, 807–810.

[22] Junttila MR and Evan GI (2009). p53–a Jack of all trades but master of none. *Nat Rev Cancer* **9**, 821–829.

[23] Brozovic A and Osmak M (2007). Activation of mitogen-activated protein kinases by cisplatin and their role in cisplatin-resistance. *Cancer Lett* **251**, 1–16.

[24] Sanchez-Perez I, Murguia JR, and Perona R (1998). Cisplatin induces a persistent activation of JNK that is related to cell death. *Oncogene* **16**, 533–540.

[25] Mansouri A, Ridgway LD, Korapati AL, Zhang Q, Tian L, Wang Y, Siddik ZH, Mills GB, and Claret FX (2003). Sustained activation of JNK/p38 MAPK pathways in response to cisplatin leads to Fas ligand induction and cell death in ovarian carcinoma cells. *J Biol Chem* **278**, 19245–19256.

[26] Brozovic A, Fritz G, Christmann M, Zisowsky J, Jaehde U, Osmak M, and Kaina B (2004). Long-term activation of SAPK/JNK, p38 kinase and fas-L expression by cisplatin is attenuated in human carcinoma cells that acquired drug resistance. *Int J Cancer* **112**, 974–985.

[27] Koyama T, Mikami T, Koyama T, Imakiire A, Yamamoto K, Toyota H, and Mizuguchi J (2006). Apoptosis induced by chemotherapeutic agents involves c-Jun N-terminal kinase activation in sarcoma cell lines. *J Orthop Res* **24**, 1153–1162.

[28] Levresse V, Marek L, Blumberg D, and Heasley LE (2002). Regulation of platinum-compound cytotoxicity by the c-Jun N-terminal kinase and c-Jun signaling pathway in small-cell lung cancer cells. *Mol Pharmacol* **62**, 689–697.

[29] Hayakawa J, Depatie C, Ohmichi M, and Mercola D (2003). The activation of c-Jun NH2-terminal kinase (JNK) by DNA-damaging agents serves to promote drug resistance via activating transcription factor 2 (ATF2)-dependent enhanced DNA repair. *J Biol Chem* **278**, 20582–20592.

[30] Tundo GR, Sbardella D, Ciaccio C, De Pascali S, Campanella V, Cozza P, Tarantino U, Coletta M, Fanizzi FP, and Marini S (2015). Effect of cisplatin on proteasome activity. *J Inorg Biochem* **153**, 253–258.

[31] Gatti L, Hoe KL, Hayles J, Righetti SC, Carenini N, Bo LD, Kim DU, Park HO, and Perego P (2011). Ubiquitin-proteasome genes as targets for modulation of cisplatin sensitivity in fission yeast. *BMC Genomics* **12**, 1–11.

[32] Bravo-Cuellar A, Hernandez-Flores G, Lerma-Diaz JM, Dominguez-Rodriguez JR, Jave-Suarez LF, De Celis-Carrillo R, Aguilar-Lemarroy A, Gomez-Lomeli P, and Ortiz-Lazareno PC (2013). Pentoxifylline and the proteasome inhibitor MG132 induce apoptosis in human leukemia U937 cells through a decrease in the expression of Bcl-2 and Bcl-XL and phosphorylation of p65. *J Biomed Sci* **20**, 13.

[33] Fennell DA, Chacko A, and Mutti L (2007). BCL-2 family regulation by the 20S proteasome inhibitor bortezomib. *Oncogene* **27**, 1189–1197.

[34] Yu H, Lee H, Herrmann A, Buettner R, and Jove R (2014). Revisiting STAT3 signalling in cancer: new and unexpected biological functions. *Nat Rev Cancer* **14**, 736–746.

[35] Xu YH and Lu S (2014). A meta-analysis of STAT3 and phospho-STAT3 expression and survival of patients with non-small-cell lung cancer. *Eur J Surg Oncol* **40**, 311–317.

[36] Kummar S, Chen HX, Wright J, Holbeck S, Millin MD, Tomaszewski J, Zweibel J, Collins J, and Doroshow JH (2010). Utilizing targeted cancer therapeutic agents in combination: novel approaches and urgent requirements. *Nat Rev Drug Discov* **9**, 843–856.

[37] DeVita Jr VT, Young RC, and Canellos GP (1975). Combination versus single agent chemotherapy: a review of the basis for selection of drug treatment of cancer. *Cancer* **35**, 98–110.

[38] Zinn RL, Gardner EE, Dobromilskaya I, Murphy S, Marchionni L, Hann CL, and Rudin CM (2013). Combination treatment with ABT-737 and chloroquine in preclinical models of small cell lung cancer. *Mol Cancer* **12**, 16.

[39] Schoenwaelder SM, Jarman KE, Gardiner EE, Hua M, Qiao J, White MJ, Josefsson EC, Alwis I, Ono A, and Willcox A, et al (2011). Bcl-xL-inhibitory BH3 mimetics can induce a transient thrombocytopathy that undermines the hemostatic function of platelets. *Blood* **118**, 1663–1674.

[40] Schmid D, Jarvis GE, Fay F, Small DM, Greene MK, Majkut J, Spence S, McLaughlin KM, McCloskey KD, and Johnston PG, et al (2014). Nanoencapsulation of ABT-737 and camptothecin enhances their clinical potential through synergistic antitumor effects and reduction of systemic toxicity. *Cell Death Dis* **5**, e1454.

[41] Cang S, Iragavarapu C, Savooji J, Song Y, and Liu D (2015). ABT-199 (venetoclax) and BCL-2 inhibitors in clinical development. *J Hematol Oncol* **8**, 129.